# Comparative Measurement of Rayleigh Scattering in Single-Mode Optical Fibers Based on an OTDR Technique

M. E. Fermann
S. B. Poole
D. N. Payne
F. Martinez

Reprinted from
JOURNAL OF LIGHTWAVE TECHNOLOGY
Vol. 6, No. 4, April 1988

# Comparative Measurement of Rayleigh Scattering in Single-Mode Optical Fibers Based on an OTDR Technique

M. E. FERMANN, S. B. POOLE, D. N. PAYNE, AND F. MARTINEZ

*Abstract*—**A new technique for comparing the Rayleigh scattering coefficients of single-mode step index fibers is described and its theoretical limitations are discussed. The validity of the technique is proven using telecommunications-grade fibers. Of particular interest is the variation of scatter found with increasing core index. In addition, the influence of small ( <0.1 percent) quantities of rare-earth dopant ions on the fiber scatter losses is analyzed for the first time.**

## I. Introduction

TELECOMMUNICATIONS fibers are now being produced in which the losses approach the intrinsic Rayleigh scatter loss of pure $SiO_2$ [1]. However, although such ultralow loss fibers have been fabricated in the laboratory their routine fabrication in a production environment is proving more difficult. A technique which can easily separate the scatter loss in a fiber from any other loss sources (e.g., hydroxyl absorption or waveguide imperfections) is therefore required. Similarly, in the development of fibers for use at longer wavelengths where the Rayleigh scattering contribution to the loss is lower [2], a simple technique which can separate this scatter loss from the total fiber loss is also required. More recently, fibers doped with small amounts of rare-earth ions have become available [3], [4] in which it has been suggested that the increased loss of such fibers may be due to increased scatter caused by the presence of relatively large rare-earth ions within the glass matrix.

To date, several techniques have been proposed for the measurement of Rayleigh scattering loss $\alpha_s$ in optical fibers. These include microcalorimetry [5]-[8] the use of integrating spheres [9] or cubes [10], [11], and a comparison of Brillouin and Rayleigh scattering [12]. In addition, the $\lambda^{-4}$ dependent component of the fiber spectral attenuation may be used to obtain $\alpha_s$ in multimode fibers [13], [14]. However, this technique can not be applied to single-mode fibers since their wavelength dependent losses due to geometrical imperfections are not generally known [15]. All the above techniques suffer from the limitations that they are either applicable only to multimode fibers or do not give the scatter at the wavelength of operation of the fiber. Consequently, a simple technique which can measure $\alpha_s$ in low-loss single-mode fiber operating at 1.3 or 1.55 $\mu$m is required.

To this end, we present a new technique based on optical time domain reflectometry (OTDR) that has been developed for the simple accurate relative measurement of $\alpha_s$ in single-mode optical fibers. The theory of the technique is developed and the sources of error in the measurement are analyzed. Results are presented for both standard telecommunications fibers and for fibers containing rare-earth impurity dopant ions. These show firstly that the (concentration of $GeO_2$)$^{1/2}$ dependence of scatter losses noted in multimode fibers [14] also holds for single-mode fibers and secondly that the incorporation of small amounts ( <0.1 percent) of rare-earth dopant ions into the fiber core does not affect the fiber scatter losses. The extension of the technique to more complex fiber designs is discussed.

## II. Theory

In OTDR, a short optical pulse launched into an optical fiber is both scattered and attenuated as it propagates along the fiber. A small fraction of the scattered power is guided backwards and monitored by a detector. The power returning to the detector $P(t)$ is given by

$$P(t) = P_0 W \eta(z) \exp\left(-\int_0^t \alpha(z) V_g \, dt\right) \tag{1}$$

where $P_0$ is the launched power, $W$ the pulsewidth, $\alpha$ the attenuation, and $\eta$ is the backscatter factor [16], [17] of the fiber, given by

$$\eta = 0.5 V_g \alpha_s B(z). \tag{2}$$

Here $V_g$ is the group velocity, $\alpha_s$ the Rayleigh scatter coefficient, and $B(z)$ the backscatter capture fraction.

Provided both the backscatter capture fraction $B(z)$ and $V_g$ are known, it is possible to determine a value for $\alpha_s$ by comparing the launched power with the backscattered power [18]. However, an accurate comparison of the forward and backward going pulses is difficult owing to the large dynamic difference in power levels, which typically exceeds 50 dB.

A simpler technique is therefore required. This will be described with reference to Fig. 1 which shows an idealized backscatter trace. Here, a high-quality low-loss fiber

Manuscript received February 10, 1987.

The authors are with the Department of Electronics and Information Engineering, Southampton University, Southampton 509 5NH, U.K.

IEEE Log Number 8718508.

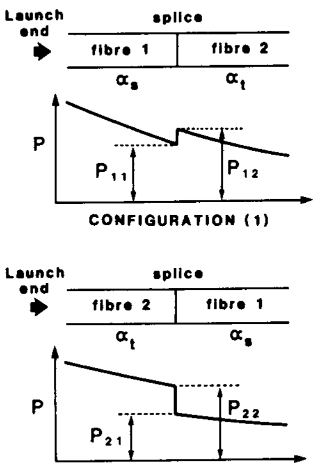


Fig. 1. The two launch configurations and idealized backscatter traces for a measurement of the relative scatter coefficients of fibers 1 and 2. The coefficients $P_{11}$, $P_{12}$ are the backscattered light powers from fibers 1 and 2 at the splice in configuration 1, and $P_{21}$, $P_{22}$ refer to the backscattered light powers from fibers 2 and 1 in configuration 2, respectively.

is used as a reference fiber to which is spliced the fiber under test. The ratio of the backscattered powers at the splice, using the test and standard fiber in turn as a launch fiber, are then compared. Using (1) and (2), it can be shown that the ratio $R_1 = P_{12}/P_{11}$ is given by

$$R_1 = \frac{V_{g2}}{V_{g1}} \frac{\alpha_{s2}}{\alpha_{s1}} \frac{B_2(z_0)}{B_1(z_0)} T^2 \tag{3}$$

where $P_{11}$, $P_{12}$ are the backscattered powers at the splice due to fibers 1 and 2, $B_1(z_0)$, $B_2(z_0)$ are the corresponding capture fractions at the splice, and $T$ is the power transmission coefficient of the splice. $T$ can be measured either by a cutback technique or by obtaining a backscatter trace from both sides of the splice [19]. In the latter case $T$ is given by

$$T = (R_1 R_2)^{1/4} \tag{4}$$

where $R_2 = P_{21}/P_{22}$ is the ratio of the backscattered powers as measured using fiber 2 as the launch fiber. It remains, therefore, to determine $V_g$ and $B(z_0)$.

For weakly guiding [20] single-mode step index fibers with $\Delta = (n_{co} - n_{cl})/n_{co} << 1$ percent, where $n_{co}$, $n_{cl}$ are the core and cladding refractive indices, it is sufficiently accurate to write $V_g = c/n_{co}$. Here $c$ is the vacuum velocity of light. For normalized frequencies ($V$-values) $V > 1.7$, the error introduced by this approximation is typically less than 0.3 percent. Similarly, for these fibers the mode field may be approximated to a high accuracy by a Gaussian function [21]. Assuming a uniform scatter loss distribution across the mode fields, $B(z)$ is then given by [17]

$$B = 6/(Kn_{co}\omega)^2 \tag{5}$$

where $K = 2\pi/\lambda$ and $\omega$ is the Marcuse spot size [21] defined as the $1/e^2$ power diameter of the Gaussian function obtained by maximizing the launch efficiency integral.

It is clear therefore that the ratio of the Rayleigh scatter coefficients may be written using (3)–(5) and the approximations for $V_{g1}$ and $V_{g2}$ as

$$\frac{\alpha_{s1}}{\alpha_{s2}} = \left(\frac{R_2}{R_1}\right)^{1/2} \left(\frac{n_1}{n_2}\right)^3 \left(\frac{\omega_1}{\omega_2}\right)^2 \tag{6}$$

where $n_1$, $n_2$ are the core refractive indices of fibers 1 and 2. The ratio of the scatter coefficients of two fibers can thus be obtained by a backscatter measurement from both ends of the jointed fibers and a knowledge of their spot sizes.

The validity of the assumptions used to derive (6) are analyzed in Appendix I. This shows that for $V$-values $>2$ any errors introduced are negligible and may therefore be ignored in practice.

## III. Measurements

The experimental arrangement for backscatter measurements is shown schematically in Fig. 2. Here, fiber 1 is the reference and fiber 2 is the fiber to be compared to it. A fusion splice was used to join the two fibers as this gave greater stability during the measurement than a simple butt splice. Errors due to detector saturation from Fresnel reflections from the launch end of the fiber were reduced by incorporating either an acoustooptic deflector to blank off the initial signal [22] or a suitable relay fiber to allow the detector to recover from the initial saturation.

The coefficients $R_i$ in (6) are obtained by fitting exponential curves to the backscatter traces before and after the splice and hence determining the power ratio at the splice. Since the measurement of the coefficients $R_i$ is independent of the splice losses, relatively bad splices may be tolerated, limited only by the dynamic range and the linearity of the measurement system. An extremely poor splice may, however, have apparent additional losses due to excitation of the lossy $LP_{11}$ mode. To minimize any errors arising from this, the first few measurement points on either side of the splice are discarded when using the fitting routine.

To obtain maximum accuracy under varying measurement conditions, the OTDR resolution and launch power must be matched to the fiber loss; higher fiber loss requiring shorter, high-power pulses to maintain the accuracy obtained for long lengths of low-loss telecommunications-grade fibers. In our experiments pulses of between 15 and 400 ns were used, corresponding to a fiber length resolution between 3 and 75 m. The high spatial resolution measurements were performed using a pulsed dye laser system operating at wavelengths of 640 nm and 1 $\mu$m with the lower resolution results obtained at a wavelength of 1.3 $\mu$m, using a commercial OTDR system [23]. With the dye laser up to 2500 and for the 1.3 $\mu$m measurement up to $1 \times 10^6$ waveforms were averaged to achieve a measurement accuracy of 1 percent for the coefficients $R_i$.

The equivalent-step-index value of $\Delta$ for the fiber core was calculated from measurements of the fiber refractive index profile using the refracted near-field technique [23],

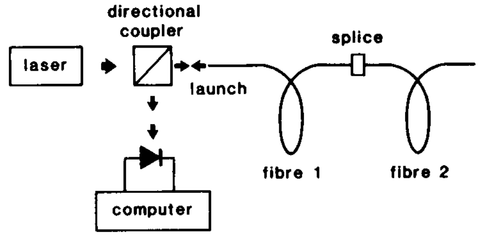


Fig. 2. Arrangement for measurement of backscatter traces. Each end is used consecutively as the launch.

[24]. For experimental convenience, the spot sizes were obtained using the (1/2) truncated least-square-fitted power transmission transverse offset technique [25]. Since (6) requires only relative measurements of the spot sizes, no absolute calibration of the equipment was necessary. However, the measurement repeatability was checked and found to have a standard deviation $\sigma$ of 0.1 $\mu$m. In addition, owing to the data fitting routine used to obtain the "best" Gaussian fit, $V$-value-dependent standard errors of up to 1 percent in the range $1.76 < V < 2.64$ are introduced [25]. However, since only the ratio of the spot sizes is required, these standard errors tend to cancel giving a typical residual standard error of < 1 percent, which is within the repeatability of the measurement discussed above. Thus, for a typical telecommunications fiber with a mode field diameter of 10 $\mu$m it is estimated that the relative scatter loss may be obtained to within 5-percent accuracy. Assuming a scatter loss of 0.3 dB/km at 1.3 $\mu$m, differences of 0.015 dB/km of scatter loss may therefore be detected.

Two series of investigations were carried out using this technique. Firstly, the effects of $GeO_2$ concentration on the Rayleigh scatter in telecommunications fiber operating at 1.3 $\mu$m was investigated. This was intended to both compare the accuracy of the technique to previously publish results and also to gain experience in the measurements. An investigation of possible excess scattering loss due to the introduction of low levels of rare-earth ions into the fiber [4] was then undertaken.

## IV. Results

### A. Telecommunications Grade Fibers

The first part of the measurements was aimed at investigating the effects of $GeO_2$ concentration on the Rayleigh scatter levels of standard single-mode step-index telecommunications fibers at their design wavelength of 1.3 $\mu$m. Six fibers were used in this study and their properties are summarized in Table I. Fibers 1–3 were manufactured by Pirelli General plc using the VAD process and fibers 4–6 were manufactured with the MCVD process by Pirelli General, York VSOP, and Southampton University, respectively. The fiber refractive index profiles are shown in Fig. 3. All fibers had a $GeO_2$-doped silica core, an approximately matched silica or phosphorus flourine doped cladding and were operated at $V$-values between 2.2 and 2.3 to minimize the error due to inhomogeneous radial scatter distribution (Appendix 1). Fiber 1 was chosen as

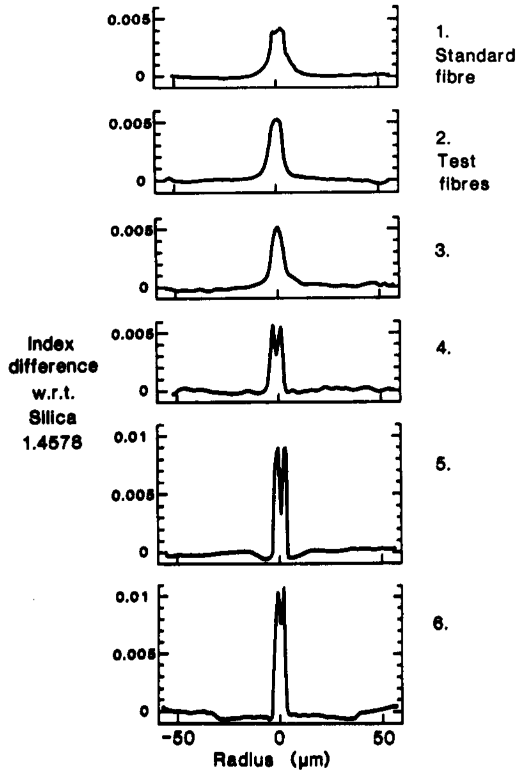


Fig. 3. Refractive index profiles of the telecommunications fibers used in the measurements. Fiber 1 is the reference fiber. Fibers 1–4 have a matched cladding while that of fibers 5 and 6 is slightly depressed.

TABLE I
SUMMARY OF TELECOMMUNICATION FIBER PROPERTIES
(Fiber 1 is the standard fiber and fibers 2–6 are the test fibers)

| Fibre | NA | $\alpha$ / dB/km | Manufacturing process |
|---|---|---|---|
| 1 | .10 | .39 | VAD |
| 2 | .12 | .54 | VAD |
| 3 | .12 | .56 | VAD |
| 4 | .13 | .60 | MCVD |
| 5 | .15 | .64 | MCVD |
| 6 | .17 | .70 | MCVD |

the standard fiber, since it exhibited the lowest total loss of 0.39 dB/km and the scatter levels of the other fibers were compared to this.

The results of the scatter measurements are plotted in Fig. 4 as relative scatter levels against fiber NA. The error bars here were estimated from the measurement accuracy of the coefficients $R_i$ and the mode field diameters. Within this measurement accuracy the scatter levels are found to be linearly dependent on the numerical aperture of the fibers for NA-values ranging from 0.10 to 0.17. These results compare well to measurements made by other workers [14] on $GeO_2$-doped multimode fibers, where generally higher $GeO_2$ doping levels were considered.

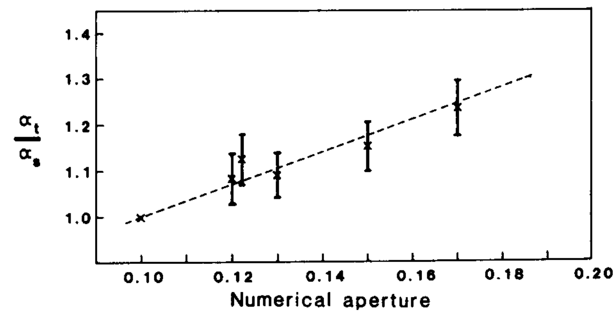


Fig. 4. Dependence of $\alpha_t/\alpha_s$, i.e., the ratio of the scatter loss of single-mode step-index $GeO_2$ doped silica fibers to that of a reference fiber, plotted as a function of numerical aperture. An approximately linear dependence of scattering on numerical aperture is observed for the range investigated.

## B. Rare-Earth-Doped Fibers

To the authors knowledge, no exact measurements have ever been made on the scattering performance of rare-earth impurity dopants in glass. The obvious problems here are the high absorption losses due to the concentration of rare-earth ions incorporated into the glass, which leads in turn to a reduced scattered light power and difficulties in calibration. With the recent production of rare-earth-doped fibers [4], these problems could be partially overcome. As may be seen in Fig. 5, despite absorption bands with losses of typically several 10 000 dB/km per 100 ppm of the impurity dopant there remain low-loss windows with an attenuation of only a few decibels per kilometer. However, the question arises as to why the total loss does not reduce to that of pure $SiO_2/GeO_2$ fibers outside these absorption bands. It has previously been suggested that this additional loss is due to increased scattering from the rare-earth ions within the glass matrix [4].

To investigate this, two $Nd^{3+}$ doped fibers were chosen as representative of typical rare-earth-doped fibers and their scatter levels were compared to those of undoped fibers of similar design. The fiber properties are summarized in Table II. The large variation in fiber properties evident here is due to the $Nd^{3+}$ doped fibers having different design considerations to telecommunications fibers. Nevertheless, it transpires even for this range of $\Delta$ values, the measurement accuracy is limited only by that of the mode field diameter measurements. The measurements were carried out at both 640 nm and 1 $\mu$m, and the results are shown in Table III. The ratios of the scatter coefficients are given both as determined experimentally and as extrapolated from the measurements on the telecommunication fibers 1-6. It can be seen that within the measurement accuracy (which here was about 10 percent, due to the smaller spot sizes that had to be measured than for the telecommunications fibers) the incorporation of several 100 ppm of $Nd^{3+}$ into silica does not lead to an increase in $\alpha_s$. This indicates that at the dopant concentrations encountered in these fibers, the $Nd^{3+}$ ions are incorporated interstitially within the silica matrix. The small increase in loss outside the absorption bands noted previously is therefore due to residual "tails" of these absorption bands.

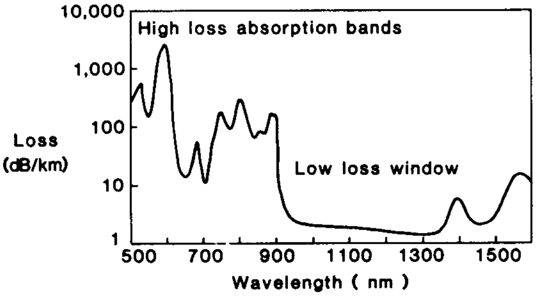


Fig. 5. Absorption spectrum of a silica fiber doped with 30 ppm $Nd^{3+}$ Note the low-loss absorption window between 950 and 1350 nm, where the absorption is only about 1 dB/km higher than in standard telecommunications fibers.

TABLE II
SUMMARY OF $Nd^{3+}$ DOPED AND UNDOPED REFERENCE FIBER PROPERTIES ($\alpha$ = total loss at the measurement wavelength $\lambda$, $[Nd^{3+}]$ is the $Nd^{3+}$ concentration in the fiber in parts per million.)

| Fibre | NA | $\alpha$ (dB/km) | $\lambda$ ($\mu$m) | $[Nd^{3+}]$ (ppm) |
|---|---|---|---|---|
| 7 | .14 | 11 | .64 | -- |
| 8 | .09 | 22 | .64 | 30 |
| 9 | .11 | 3 | 1.00 | -- |
| 10 | .21 | 14 | 1.00 | 300 |

TABLE III
THE SCATTER LOSS RATIOS $\alpha_i/\alpha_j$ OF $Nd^{3+}$ DOPED AND UNDOPED SILICA FIBERS COMPARED TO THE SCATTER LOSS RATIO AS ESTIMATED FROM (9)

| Fibre | Scatter loss ratios $\alpha_i/\alpha_j$ Measured | $\alpha_i/\alpha_j$ Predicted |
|---|---|---|
| Fibre 7 / Fibre 8 | 1.22 | 1.18 |
| Fibre 9 / Fibre 10 | 0.70 | 0.74 |

In addition, the temperature dependence of the scatter levels of $Nd^{3+}$-doped fibers was investigated by heating the standard and test fibers in turn and was found to be

$$\frac{1}{\alpha_s}\frac{d\alpha_s}{dT} = 0.016 \text{ percent } {}^0C^{-1}. \quad (7)$$

This is the same figure as measured for silica fibers and is due solely to the temperature dependence of the backscatter capture fraction [26].

## V. Discussion

Two mechanisms are known to lead to the observed increase in Rayleigh scattering with increasing $GeO_2$ concentration in the fiber. The first effect is the higher scattering due to density fluctuations in $GeO_2$ as compared to $SiO_2$ [27]. Secondly, the random statistical distribution of $GeO_2$ in $SiO_2$ leads to additional small variations of the dielectric constant and hence to concentration scattering [11]. From Fig. 4 and the well-known dependence of refractive index on $GeO_2$-concentration [28], we may write for the relative Rayleigh scatter coefficient of the $SiO_2$–$GeO_2$ binary system

$$\alpha_s/\alpha_t = 1 + 2.3(C_t^{1/2} - C_s^{1/2}) \tag{8}$$

where $\alpha_s$, $\alpha_t$ are the scatter losses, and $C_s$ and $C_t$ are the $GeO_2$ concentrations in the standard and test fiber, respectively. An upper limit for the scatter loss of fiber 1, $\alpha_s'$ is given by

$$\alpha_s' = \alpha_{tot} - \alpha_{OH} \tag{9}$$

where $\alpha_{tot}$ is the total fiber loss and $\alpha_{OH}$ is the excess loss due to hydroxyl impurities which may be calculated from the intensity of the absorption peak at 1390 nm [13]. From spectral attenuation measurements, the hydroxyl concentration in fiber 1 was found to be 90 ppb which gives $\alpha_{OH} = 0.08$ dB/km. From Table I, $\alpha_{tot} = 0.39$ dB/km and hence $\alpha_s' = 0.31$ dB/km.

Substituting this value into (8) allows the calculation of upper limits to the scatter losses $\alpha_{max}'$ of fibers 2–6. These are shown in Table IV along with values of $\alpha_t$ calculated using (8). It may be seen that scatter losses and hydroxyl absorption do not totally explain the higher total losses of fibers with high $GeO_2$ concentration. The reasons for this are not entirely clear and may be attributable to excess losses caused by specific manufacturing conditions.

The undetectable scatter loss due to the presence of rare-earth ions within the host silica matrix suggests that higher doping levels than presently demonstrated with negligible increase in scatter losses, are possible. For very-high doping levels, however, it is expected that the silica matrix will be modified, thus leading to increased scattering due to the presence of relatively large $Nd_2O_3$ molecules. The technique described here may then provide valuable information about the structure of such glasses. The high attenuation levels expected, however, may require a high resolution OTDR [29] to obtain acceptable measurement accuracy.

A reduction in measurement time may be obtained, if required, by simultaneously measuring the backscatter traces for test fibers using the arrangement of Fig. 6. Here fiber *B* is the reference fiber and fibers A and C are used in turn as the launch fiber. Thus for each relative measurement of $\alpha_s/\alpha_t$ only one splice must be made and one measurement each of spot size, refractive-index profile, and backscatter trace need be obtained.

TABLE IV
THE UPPER LIMIT FOR THE SCATTER LOSSES OF THE FIBERS AS CALCULATED USING (9) ARE SHOWN
($\alpha_{max}'$ is the total loss minus hydroxyl absorption, $[GeO_2]$, $[OH^-]$ represent $GeO_2$ and OH concentrations.)

| Fibre | $[GeO_2]$ | $[OH^-]$ | $\alpha_{max}'$ | $\alpha_t$ |
|---|---|---|---|---|
| | % | ppb | dB/km | dB/km |
| 1 | 2.3 | 90 | .31 | .31 |
| 2 | 3.5 | 220 | .36 | .34 |
| 3 | 3.5 | 220 | .38 | .34 |
| 4 | 4.0 | 130 | .39 | .34 |
| 5 | 5.3 | 30 | .62 | .37 |
| 6 | 6.8 | 220 | .52 | .39 |

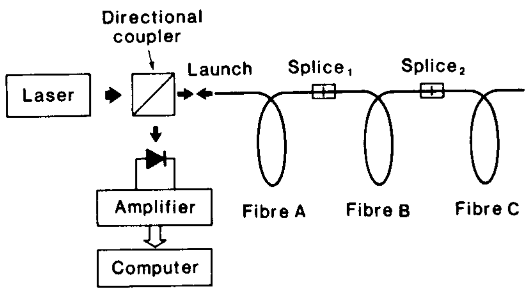


Fig. 6. Suggested experimental arrangement to measure the relative scatter coefficients of two fibers simultaneously. Fiber *B* is the standard fiber and fibers *A* and *C* are the test fibers.

In addition to the relative scatter loss of quasi step-index fibers described above, the scatter loss of fibers with an arbitrary index profile may in principle be measured, provided the light power distribution in the fiber is known with sufficient accuracy. The backscatter capture fraction may then be calculated using (10) and $\alpha_s$ obtained as described above.

## VI. Conclusions

The idea of a standard reference fiber in conjunction with an OTDR-technique has been introduced for the measurement of Rayleigh scattering in single-mode optical fibers. The technique for the accurate comparison of a test fiber to this reference fiber has been described and a detection capability of less than 0.015 dB/km of scatter loss difference at 1.3 $\mu$m estimated. The increase of scatter losses with core $GeO_2$ concentration has been observed and this underlines its importance for the optimum design of optical fibers. The effect on fiber scatter losses of the addition of small amounts of $Nd^{3+}$ ions to the fiber core was also investigated and found to be negligible.

The theoretical minimum Rayleigh scatter loss in silica optical fibers has not yet been achieved in the manufacturing process [1]. A careful application of the present measurement technique may thus prove valuable in finding parameters to optimize fiber production.

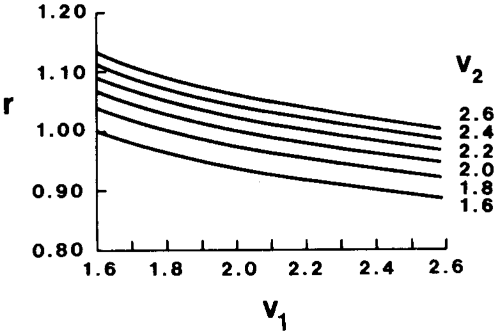


Fig. 7. Theoretical accuracy of the Gaussian approximation for the ratio $B_2(V_2)/B_1(V_1)$, i.e., the ratio of the backscatter capture fractions for two fibers with different $V$-values, calculated from (10) for uniform scatter loss distributions.

## Appendix I
## The Effects of Non-Gaussian Fields and Inhomogeneous Scatter Loss Distribution

As pointed out in Section II, (6) is only exact for Gaussian fields and uniform scatter loss distributions. Using the exact form of the backscatter capture fraction [17]

$$B = \frac{3\,NA^2}{4n_{co}^2 V^2} \frac{\int_0^\infty R\alpha_s(R)\,\psi_N^4(R)\,dR}{\int_0^\infty R\alpha_s(R)\,\psi_N^2(R)\,dR \int_0^\infty R\psi_N^2(R)\,dR} \quad (10)$$

where $\psi_N(R)$ is the field distribution in the fiber as a function of radius, the accuracy of (6) may be evaluated. Fig. 7 plots the error for $\alpha_{s1}/\alpha_{s2}$ for a constant scatter loss distribution in a step index fiber as a function of $V_1$ and $V_2$. Here

$$r = \left(B_2(V_2)/B_1(V_1)\right)_g / \left(B_2(V_2)/B_1(V_1)\right)_{\text{exact}} \quad (11)$$

is the ratio of the Gaussian approximation for $(B_2(V_2)/B_1(V_1))_g$ over its exact form. For $V_1 = V_2$ the ratio $r = 1$ and (6) is exact. However, about 1-percent error is introduced per 0.1 difference in $V$-value between the two fibers. For most applications, only the comparison of fibers near $LP_{11}$ mode cutoff is of interest (i.e., $V_1 = V_2 \approx 2.3$) and thus this error may then be neglected.

For nonuniform scatter loss distributions $\alpha_s$ may be defined as the weighted average of the scatter over the modal field [17]. However, in practice $\alpha_{co}$ and $\alpha_{cl}$, the scatter loss in the fiber core and cladding, may each be assumed to be constant and the scatter loss of the fiber may be approximated by $\alpha_{co}$. Thus, due to the implicit dependence of $B$ on the scatter loss distribution, small errors are introduced in (6) when using this approximation. Fig. 8 plots the parameter $r$ (assuming Gaussian fields) as a function of $V_1$ and $V_2$, where $r$ is given by

$$r = \left(B_2(V_2)/B_2(V_1)\right)_{\text{approx}} / \left(B_1(V_2)/B_1(V_1)\right)_{\text{exact}}. \quad (12)$$

Here the extreme case is assumed that for fiber 1 $(\alpha_{cl}/\alpha_{co}) = 0.5$ and for fiber 2 $(\alpha_{cl}/\alpha_{co}) = 2$. For $V = 2.4$, the

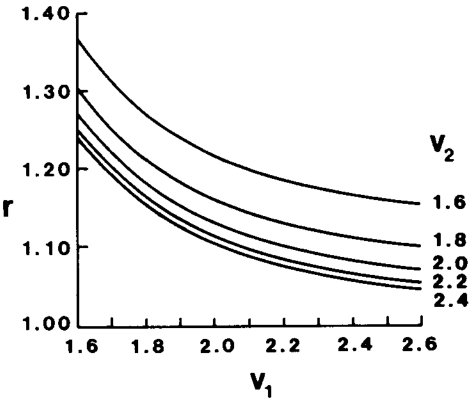


Fig. 8. Theoretical accuracy of (6) for the scatter loss ratio of two fibers that exhibit significantly different scatter loss coefficients for core and cladding. Here the assumed values for the ratio of the scatter loss coefficients of core and cladding are: $(\alpha_{cl}/\alpha_{co})_1 = 0.5$ for fiber 1 and $(\alpha_{cl}/\alpha_{co}) = 2$ for fiber 2.

error in (6) is less than 6 percent compared to a difference in the ratios of $(\alpha_{cl}/\alpha_{co})_1$, and $(\alpha_{cl}/\alpha_{co})_2$ of 400 percent. For smaller $V$-values the error increases, but it remains below 15 percent for $V_1$, $V_2 > 2$. Thus the effect of nonuniform scatter loss distribution is relatively small and may be neglected in (6).

## References

[1] R. D. Maurer, "Optical properties of fiber optic materials," *J. Non-Crystalline Sol.*, vol. 47, pp. 135–146, 1982.
[2] T. Miyashita and T. Manabe, "Infrared optical fibers," *IEEE Trans. Microwave Theory Tech.*, vol. MTT-30, pp. 1420–1427, 1982.
[3] S. B. Poole, D. N. Payne, and M. E. Fermann: "Fabrication of low-loss optical fibers containing rare-earth ions," *Electron. Lett.*, vol. 21, pp. 737–738, 1985.
[4] S. B. Poole, D. N. Payne, R. J. Mears, M. E. Fermann, and R. I. Laming, "Fabrication and characterization of low-loss optical fibers containing rare-earth ions," *J. Lightwave Technol.*, vol. LT-3, pp. 870–876, 1986.
[5] A. Zaganiaris, "Simultaneous measurement of absorption and scattering losses in bulk glass and optical fibers by a microcalorimetric method," *Appl. Phys. Lett.*, vol. 25, pp. 345–347, 1974.
[6] R. L. Cohen, "Loss measurements in optical fibers, 1: Sensitivity limit of bolometric techniques," *Appl. Opt.*, vol. 13, pp. 2518–2521, 1974.
[7] R. L. Cohen, "Loss measurements in optical fibers, 2: Bolometric measuring instrumentation," *Appl. Opt.*, vol. 13, pp. 2522–2526, 1974.
[8] F. T. Stone, W. B. Gardner, and C. R. Lovelace, "Calorimetric measurement of absorption and scattering loss in optical fibers," *Opt. Lett.*, vol. 2, pp. 48–50, 1978.
[9] D. B. Keck, P. C. Schultz, and F. Zimar, "Attenuation of multimode glass optical waveguides," *Appl. Phys. Lett.*, vol. 21, pp. 215–217, 1972.
[10] A. R. Tynes, "Integrating cube scattering detector," *Appl. Opt.*, vol. 9, pp. 2708–2710, 1970.
[11] W. A. Gambling *et al.* "Optical fibers based on phosphosilicate glass," *Proc. Inst. Elec. Eng.*, vol. 123, pp. 570–575, 1976.
[12] T. C. Rich and D. A. Pinnow, "Total optical attenuation in bulk silica," *Appl. Phys. Lett.*, vol. 20, pp. 264–265, 1972.
[13] R. D. Maurer, "Glass research for optical waveguides," *J. Non-Crystalline Sol.*, vol. 42, pp. 197–208, 1980.
[14] H. Murata, S. Inao, Y. Matsuda, and T. Kuroha, "Optimum design for optical fiber used in optical cable systems," in *Proc. 4th Eur. Conf. Optical Commun.* (Genoa, Italy), 1978, pp. 242–248.
[15] K. Inada, R. Yamauchi, and M. Miyamoto, "Wavelength dependence of geometrical imperfection losses in single-mode fibers," in *Proc. 8th Eur. Conf. Optical Commun.* (Cannes, France, 1982, pp. 596–600.
[16] E. Brinkmeyer, "Analysis of the backscattering method for single-

mode optical fibers," *J. Opt. Soc. Amer.*, vol. 70, pp. 1010–1012, 1980.
[17] A. H. Hartog and M. P. Gold, "On the theory of backscattering in single-mode optical fibers," *J. Lightwave Technol.*, vol. LT-2, pp. 76–82, 1984.
[18] M. P. Gold and A. H. Hartog, "Measurement of backscatter factor in single-mode fibers," *Electron. Lett.*, vol. 17, pp. 965–966, 1981.
[19] P. De Vita and U. Rossi, "The backscattering technique: Its field of applicability in fiber diagnostics and attenuation measurement," *Opt. Quantum Electron.*, vol. 12, pp. 17–22, 1980.
[20] D. Gloge, "Weakly guiding fibers," *Appl. Opt.*, vol. 10, pp. 2252–2258, 1971.
[21] D. Marcuse, "Gaussian approximation of the fundamental modes in graded index fibers," *J. Opt. Soc. Amer.*, vol. 68, pp. 103–109, 1978.
[22] M. P. Gold and A. H. Hartog, "Improved dynamic range single-mode OTDR at 1.3 μm," *Electron. Lett.*, vol. 20, pp. 285–287, 1984.
[23] York Technology, FCm1000.
[24] W. J. Stewart and D. C. J. Reid: "High resolution optical fiber index profiling," in *Proc. 8th Eur. Conf. Optical Commun.* (Cannes, France), 1982, pp. 21–24.
[25] W. T. Anderson, "Consistency of measurement methods for the mode field radius in a single-mode fiber," *J. Lightwave Technol.*, vol. LT-2, pp. 191–197, 1984.
[26] A. Hartog, "Distributed temperature sensing," *J. Lightwave Technol.*, vol. LT-1, pp. 498–509, 1983.
[27] M. E. Lines, "Scattering losses in optic fiber materials," *J. Appl. Phys.*, vol. 55, pp. 4052–4063, 1984.
[28] S. R. Norman, Ph.D. thesis, Southampton University, Southampton, U.K., 1982.
[29] D. Uttam and B. Culshaw, "Precision time domain reflectometry in optical fiber systems using a frequency modulated continuous wave ranging technique," *J. Lightwave Technol.*, vol. LT-3, pp. 971–977, 1986.

*

**Martin E. Fermann** was born in Dubrowno, Poland, on May 9, 1960. He received the M.Sc. degree from the University of Reading, England, in 1984.

In October 1984, he joined the Optical Fiber Group at Southampton University as a Research Assistant where he is working on fiber measurements.

**Simon B. Poole** was born in Watford, England, in 1958. He received the B.Sc. in electrical and electronic engineering from the University of Nottingham in 1979.

In 1981, he joined the Optical Fiber Group at Southampton University as a research student working on optical-fiber fabrication and characterization. He is now the Pirelli Research Fellow within the Group. His current research interests include novel dopant materials and their uses in fiber devices.

*

**David N. Payne** was born in Lewes, England, on August 13, 1944, and educated in Central Africa. He received the B.Sc. in electrical engineering, the Diploma in quantum electronics, and the Ph.D degree from the University of Southampton, England.

In 1972, he was appointed the Pirelli Research Fellow in the Department of Electronics, University of Southampton and in 1977 became Senior Research Fellow. He is currently Research Reader and directs the Optical Fiber Group, consisting of some 40 members. Since 1969 his research interests have been in Optical Communications and have included preform and fiber fabrication techniques, optical propagation in multimode and single-mode fibers, fiber and preform characterization, wavelength-dispersive properties of optical-fiber materials, optical-transmission measurements, and fiber devices. He has published over a 100 papers and holds 11 patents. Currently his main fields of interest are special fibers, fiber lasers and devices, fiber sensors, and optical transmission.

Dr. Payne is an Associate Editor or the JOURNAL OF LIGHTWAVE TECHNOLOGY.

*

**F. Martinez,** photograph and biography not available at time of publication.